HYDROLOGICAL PROCESSES
Hydrol. Process. **20**, 3697–3708 (2006)
Published online in Wiley InterScience
(www.interscience.wiley.com) DOI: 10.1002/hyp.6383

Incoming longwave radiation to melting snow: observations, sensitivity and estimation in northern environments

J. E. Sicart,[1,2]* J. W. Pomeroy,[3] R. L. H. Essery[1] and D. Bewley[1]

[1] *Centre for Glaciology, University of Wales Aberyswyth, UK*
[2] *GREATICE, Institut de Recherche pour le Développement (IRD), Montpellier, France*
[3] *Centre for Hydrology, University of Saskatchewan, Saskatoon, Canada*

Abstract:

At high latitudes, longwave radiation can provide similar, or higher, amounts of energy to snow than shortwave radiation due to the low solar elevation (cosine effect and increased scattering due to long atmospheric path lengths). This effect is magnified in mountains due to shading and longwave emissions from the complex topography. This study examines longwave irradiance at the snow surface in the Wolf Creek Research Basin, Yukon Territory, Canada (60°36′N, 134°57′W) during the springs of 2002 and 2004. Incoming longwave radiation was estimated from standard meteorological measurements by segregating radiation sources into clear sky, clouds and surrounding terrain. A sensitivity study was conducted to detect the atmospheric and topographic conditions under which emission from adjacent terrain significantly increases the longwave irradiance. The total incoming longwave radiation is more sensitive to sky view factor than to the temperature of the emitting terrain surfaces. Brutsaert's equation correctly simulates the clear-sky irradiance for hourly time steps using temperature and humidity. Longwave emissions from clouds, which raised longwave radiation above that from clear skies by 16% on average, were best estimated using daily atmospheric shortwave transmissivity and hourly relative humidity. An independent test of the estimation procedure for a prairie site near Saskatoon, Saskatchewan, Canada, indicated that the calculations are robust in late winter and spring conditions. Copyright © 2006 John Wiley & Sons, Ltd.

KEY WORDS longwave radiation; snowmelt; energy balance; Northern Environments; complex terrain

Received 1 August 2005; Accepted 19 January 2006

INTRODUCTION

Radiation fluxes generally account for most of the energy used in snowmelt. Net shortwave radiation is generally the dominant flux, but net longwave radiation can contribute similar, or higher, amounts of energy during cloudy periods because of the increased atmospheric emissivity (e.g. Müller, 1985; Granger and Gray, 1990; Duguay, 1993). When the snow albedo is high, snowmelt energy can be higher under cloudy skies than under clear skies (Ambach, 1974). Longwave radiation is important for the onset of snowmelt in early spring, when the solar energy is still low and the albedo of fresh snow is high. Fassnacht *et al.* (2001) showed that an accurate estimate of longwave radiation is necessary to correctly simulate stream flows resulting from snowmelt.

The longwave radiation balance of snow has received less attention than shortwave radiation, in part because of the scarcity and unreliability of measurements in mountainous regions. However, global warming preoccupations have emphasized the role of the longwave flux in the surface energy budget (e.g. Philipona

* Correspondence to: J. E. Sicart, Great Ice–IRD, Case MSE, UMII, 300, avenue du Professeur Emile Jeanbrau, 34 095 Montpellier cedex 5, France. E-mail: sicart@msem.univ-montp2.fr

et al., 2004). The variations of sky longwave radiation depend on the temperature and humidity of the atmosphere and on the cloud-cover. In rugged terrain, ground emissions enhance longwave irradiance, producing a spatial variability in snowmelt (e.g. Olyphant, 1986).

This study examines longwave irradiance at the snow surface in the Wolf Creek Research Basin, Yukon Territory, Canada, during two snowmelt seasons. The objectives are (i) to explore the potential effects of terrain emission and (ii) to derive a simple parameterization of atmospheric emission. A sensitivity study was conducted to detect the atmospheric and topographic conditions under which the surrounding terrain emission is significant. Then, we developed a simple parameterization of atmospheric longwave radiation suitable for snowmelt energy studies in open, northern environments. Cloud emission is generally calculated from observations of cloud-cover, type and altitude. However, this information is rarely available in remote locations and is subject to errors (Warren *et al*., 1985). Here, input data are from standard automatic meteorological stations: incoming shortwave radiation and air temperature and humidity. Finally, an independent test of the calculations of the atmospheric longwave radiation was conducted for a prairie site near Saskatoon, Saskatchewan, Canada.

LOCATION AND INSTRUMENTATION

The primary study site was the Wolf Creek Research Basin, located 15 km south of Whitehorse (Yukon Territory, Canada, 60°36′N, 134°57′W). The basin has a sub-arctic continental climate, characterized by a large annual variation in temperature, low humidity and low precipitation. The mean annual temperature is approximately −3 °C, with monthly mean temperatures ranging from +5 to +15 °C in summer and from −10 to −20 °C in winter. The mean annual precipitation is 350 mm, with approximately 40% falling as snow (Pomeroy and Granger, 1997). The snowmelt season generally extends from April to June.

Measurements of incoming shortwave and longwave radiation (S and L, Kipp&Zonen CM3 pyranometer and CG3 pyrgeometer), and air temperature and relative humidity (T and RH, Vaisala HMP45) were conducted over a level snow-covered tundra surface at 1430 m above sea level (a.s.l.) during two snowmelt seasons in 2002 and 2004. A Campbell 23X datalogger recorded 30-min averages of 5 s time step observations. A research camp was located near the instruments and they were cleaned shortly after any precipitation or frost occurred.

Secondary observations were conducted on snow-covered prairie grassland located 6 km south of the city of Saskatoon, Saskatchewan (52°7′N, 106°4′W) in the pre-melt and melt periods of 2004. A CNR1 radiometer and a HMP45CF hygrothermometer were used with 15 min averages 10 s observations.

The accuracy of the pyrgeometer measurements is ±10% (Halldin and Lindroth, 1992). The main source of error is interference from shortwave radiation, leading to an overestimation of the longwave signal. Corrections of L according to S, as suggested by Kipp&Zonen (1995), are site dependent (e.g. Culf and Gash, 1993; Halldin and Lindroth, 1992; Obleitner and De Wolde, 1999; Sicart *et al*., 2005). Such corrections could not be calibrated for Wolf Creek due to the lack of shaded longwave radiation measurements necessary to eliminate the interference of solar radiation. Emission from melting snow at 0 °C is sometimes used as a reference for longwave radiation measurements. In Wolf Creek, however, emission from exposed shrubs above the snow modified the emission and melting snow could not be used as a reference for L.

PARAMETERIZATION

Clear-sky radiation

As most of the sky longwave radiation received at the surface comes from the near-surface layer of the atmosphere, the clear-sky longwave irradiance in an open environment, $L_{0,\ \mathrm{clear}}$ (W m^{-2}), may be written as

$$L_{0,\ \mathrm{clear}} = \varepsilon_{\mathrm{clear}} \sigma T^4 \tag{1}$$

DOI: 10.1002/hyp

where ε_{clear} is the apparent clear-sky emissivity, $\sigma = 5{\cdot}67 \times 10^{-8}$ W m^{-2} K^{-4} is the Stefan–Boltzman constant, and T is the air temperature near the ground (K). Numerous empirical parameterizations of ε_{clear} have been proposed as a function of air temperature (T), vapour pressure (e in mb) or both (see review in Brutsaert, 1982). The parameterizations are often equivalent because there is a good correlation between temperature and humidity. By integrating water vapour emissivity in a mid-latitude standard atmosphere, Brutsaert (1975) obtained

$$\varepsilon_{clear} = C(e/T)^{1/m} \tag{2}$$

with $C = 1{\cdot}24$ and $m = 7$. The parameter C depends on the relationship between vapour pressure near the ground and the profile of humidity in the atmosphere.

Cloudy sky

Longwave radiation from cloudy skies is calculated as

$$L_0 = \varepsilon_{clear} F\ \sigma T^4 \tag{3}$$

where $F \geq 1$ is the increase in the sky emissivity due to cloud emissions, generally calculated as a function of the fractional cloud-cover. A common index of cloud-cover during daytime is the atmospheric transmissivity for shortwave radiation (τ_{atm})

$$\tau_{atm} = S/S_{extra} \tag{4}$$

where S_{extra} is the theoretical shortwave irradiance at the top of the atmosphere.

The factor F in Equation (3) can be derived from observations as

$$F = L_0/[\mathrm{C}(e/T)^{1/m}\sigma T^4] \tag{5}$$

To parameterize the total sky longwave radiation, we explored the correlations between F derived from Equation (5) and different meteorological variables (T, RH and τ_{atm}, Table I).

Terrain emission

Assuming isotropic sky and terrain radiance, the surface longwave irradiance in rugged terrain is written as

$$L = V_f L_0 + (1 - V_f)\varepsilon_s\ \sigma\ {T_s}^4 \tag{6}$$

Table I. Linear correlations between cloud emissivity derived from Equation (5) ($F \geq 1$) and measurements of relative humidity (RH), atmospheric solar transmissivity (τ_{atm}) and temperature (T), as daily averages

	r^2 (X, F)[a]			r^2 (RH, τ_{atm}, F)[b]
	$X = RH$	$X = \tau_{atm}$	$X = \sigma^2(T)$[c]	$X_1 = RH$, $X_2 = \tau_{atm}$, $Y = F$
2002 ($n = 43$)	0·63	0·29	0·23	$r^2 = 0{\cdot}63$ $F = 0{\cdot}86 + 0{\cdot}55\ RH - 0{\cdot}06\ \tau_{atm}$
2004 ($n = 29$)	0·52	0·37	0·39	$r^2 = 0{\cdot}76$ $F = 0{\cdot}97 + 0{\cdot}64\ RH - 0{\cdot}46\ \tau_{atm}$
2002–2004 ($n = 72$)	0·54	0·30	0·27	$r^2 = 0{\cdot}58$ $F = 0{\cdot}94 + 0{\cdot}49\ RH - 0{\cdot}16\ \tau_{atm}$

[a] Determination coefficients of simple regressions.
[b] Determination coefficients of multiple regressions.
[c] Variance of the half-hourly values.

DOI: 10.1002/hyp

where V_f is the sky view factor (the fraction of the celestial hemisphere visible from the surface, V_f is defined normal to slope), L_o is the sky longwave irradiance (W m^{-2}), ε_s is the terrain emissivity, which is close to unity for snow and most natural surfaces (Dozier and Warren, 1982; Oke, 1987), and T_s is the effective temperature of the emitting terrain (K).

Enhancement of L by terrain emission is important when sky radiation is low (cold and dry atmosphere, high elevation), V_f is low (steep topography) and the temperature of the emitting terrain is high (snow-free faces); it will be maximal in daytime clear-sky conditions.

The relative increase of clear-sky longwave radiation by terrain emission is derived from Equations (1) and (6) as

$$[L - L_{0,\ clear}]/L_{0,\ clear} = \Delta L/L_{0,\ clear} = (1 - V_f)[\varepsilon_s\ (T_s/T)^4 - \varepsilon_{clear}]/\varepsilon_{clear} \quad (7)$$

As ε_s is close to 1, terrain emission increases L if $T_s/T > \varepsilon_{clear}^{1/4}$, corresponding to a surface temperature threshold of about $-15\,^{\circ}$C when air temperature is $T = +10\,^{\circ}$C and $\varepsilon_{clear} = 0{\cdot}7$. Terrain emission increases L because the ground has a higher emissivity than the sky.

RESULTS

Radiation fluxes during spring

Figure 1 shows the daily incoming long- and shortwave radiation fluxes and the air temperature and humidity in spring 2004. Trends were similar in 2002. Over 24-h periods, shortwave and longwave irradiances contributed similar amounts of energy. As spring progressed, incoming longwave radiation increased due to atmospheric warming and the transmission of shortwave radiation through the atmosphere decreased due to increasing atmospheric turbidity. The thickest clouds reduced shortwave irradiance by about 70%. Mean clear-sky atmospheric shortwave transmissivity was around 0·75 in spring. Owing to the cold atmosphere, air humidity was low during clear-sky conditions (Figure 1). Air temperature became positive by late April. In 2004, as in each year since the start of the observations in 2001, a warm period of intense melting in late April was interrupted by a few days of sub-freezing temperatures in early May.

Terrain emission

Figure 2 shows the results of Equation (7) in typical clear-sky daytime conditions in Wolf Creek: sky irradiance $L_{0,\ clear} \sim 200$ W m^{-2} (Figure 1) and air temperature $T = 0\,^{\circ}$C, corresponding to an apparent sky emissivity $\varepsilon_{clear} \sim 0{\cdot}65$. The results depend little on air temperatures below $10\,^{\circ}$C. The values of the contours $\Delta L/L_{0,\ clear}$ along the bottom X-axis show the longwave radiation enhancement for an emitting melting snow surface with $T_s = T = 0\,^{\circ}$C. The terrain emission is only significant, i.e. greater than the measurement uncertainties (+20%), when the sky view factor is less than 0·65 (Figure 1), corresponding to an inclined face of a valley whose slopes are at least 35°. In very narrow valleys ($V_f \sim 0{\cdot}5$), the longwave radiation enhancement is less than 30% (60 W m^{-2}).

As snowmelt progresses, the fraction of snow-free areas increases, leading to high surface temperatures ($T_s > 0\,^{\circ}$C, Figure 2). North-facing snow-covered slopes can oppose bare ground on south-facing slopes for a month in Wolf Creek (Pomeroy *et al.*, 2003), and bare ground temperatures as high as $+30\,^{\circ}$C have been measured in spring using infrared thermometers. For $T_s = +30\,^{\circ}$C, the terrain emission becomes significant for $V_f \sim 0{\cdot}85$ (Figure 2), corresponding to a valley of 25° slopes. For emitting terrain warmer than the air, sky view factors lower than 0·7 will result in a strong terrain emission of up to +40% or +80 W m^{-2} if $T_s = +30\,^{\circ}$C (Figure 2). The total longwave irradiance is not very sensitive to the temperature of emitting surfaces: a change $\Delta T_s = 10\,^{\circ}$C changes L by less than 10% for any sky view factor higher than 0·6 (Figure 2).

Terrain enhancement of L can also be significant at night due to the small emissivity of the nocturnal cold sky and despite low ground temperatures (not shown). Calculations with the empirical formula of Plüss and

DOI: 10.1002/hyp

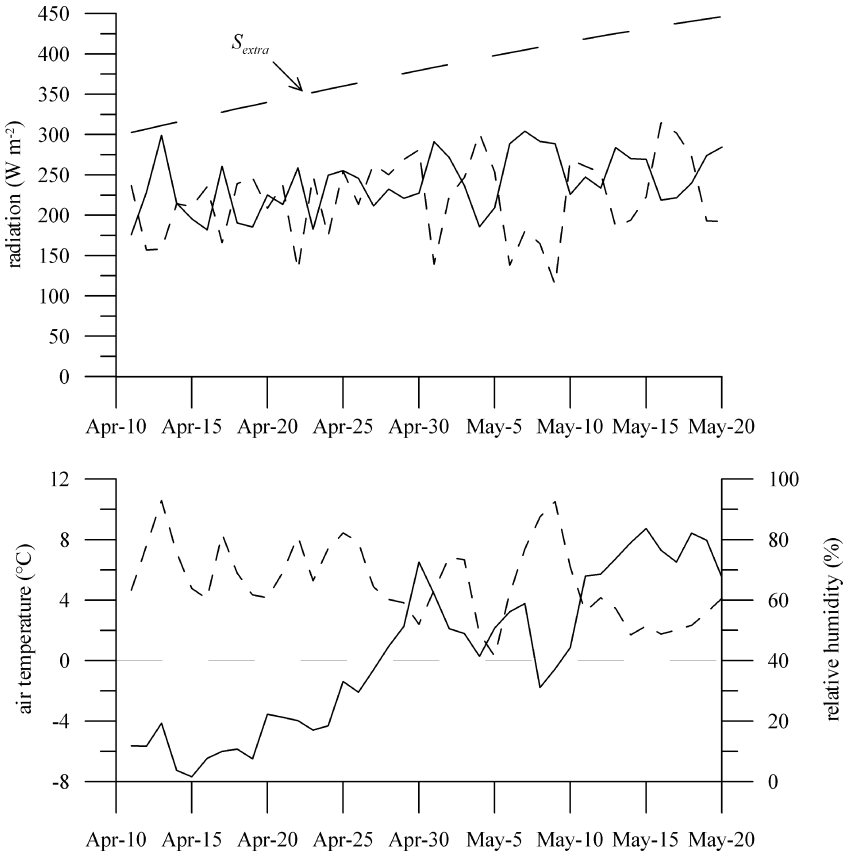

Figure 1. Upper panel: incoming longwave (solid line) and shortwave (dashed line) radiation. The theoretical solar irradiance at the top of the atmosphere is also shown (S_{extra}). Lower panel: air temperature (solid line) and relative humidity (dashed line). All data are daily averages during spring 2004

Ohmura (1997) indicated that longwave emission and transmission of the air between emitting terrain and the receiving snow surface is small in the atmospheric conditions of Wolf Creek ($\Delta L < 10$ W m^{-2}).

Clear-sky radiation

Figure 3 shows that Brutsaert's original equations (Equations (1) and (2)) agree quite well with observed minima of L corresponding to clear-sky emissions. In particular, the minimal irradiance on clear-sky nights was correctly simulated. Calculated values of L were too high on 5 May, 16 May and 17 May, 2004, but the errors remained small. The clear-sky emissivity increased steadily throughout spring as the atmosphere warmed. Emissivity fluctuations were small because the vapour pressure did not vary much. The coefficients of variation of $\varepsilon_{\text{clear}}$ and T^4 were around 6 and 10%, respectively, so the atmospheric temperature prevailed over emissivity in causing fluctuations of clear-sky longwave radiation. The correction of Brutsart's equation by Konzelmann *et al*. (1994) to account for the emissivity of greenhouse gases other than water vapour resulted in an overestimation of the clear-sky emissivity in Wolf Creek, probably because it was derived under the strong inversion conditions of the Greenland ice sheet.

As the snow-covered area decreases, the relationship between temperature and humidity near the ground and the radiative properties of the atmosphere may change, causing a bias in the calculations of sky longwave radiation. At lower elevations in the Wolf Creek Forest (750 m a.s.l.) and at the nearby Whitehorse airport (700 m a.s.l.), snow cover is depleted in early April (Sicart *et al*., 2004), before the snowmelt period at the

DOI: 10.1002/hyp

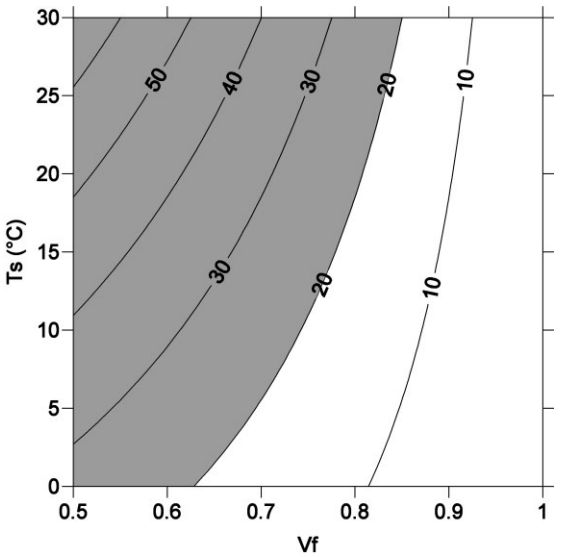

Figure 2. Relative increase of longwave irradiance due to terrain emission ($\Delta L/L_{0,\ \mathrm{clear}}$, Equation (7)) in percent according to sky view factor (V_f) and surface temperature (T_s). Areas of $\Delta L/L_{0,\ \mathrm{clear}} > 20\%$ are shaded. The air temperature is $T = 0\,^{\circ}\mathrm{C}$ and the clear-sky emissivity is $\varepsilon_{\mathrm{clear}} = 0{\cdot}65$ (see text)

radiation study site at 1430 m a.s.l. (Figure 1). Thus, the clear-sky emissivity at 1430 m a.s.l. was calculated from Brutsaert's equation using observations from the lower locations (~700 m a.s.l.), with corrections for the vertical gradients of temperature (lapse rate from soundings), humidity (uniform relative humidity) and atmospheric pressure as proposed by Marks and Dozier (1979). Characteristic profiles were derived from radiosonde observations at Whitehorse airport. However, the calculations of clear-sky emissivity were not improved compared to calculations using high altitude surface observations and new sources of uncertainties appear, such as the diurnal variations of the gradients.

Cloudy sky

On the hourly time scale, τ_{atm} depends on the relative positions of the clouds and the sun and is not a good index of cloud-cover (Equation (4)). On the daily time scale, Figure 4 shows that high cloud emission factors (F from Equation (5)) were associated with low shortwave transmissivities, but the data scatter in the relationship is large. Considering that the cloudless-sky transmissivity is approximately 0·75, a polynomial fit to F is (Figure 4)

$$F \sim 1{\cdot}5 - 7/8\ {\tau_{\mathrm{atm}}}^2 \tag{8}$$

Calculations of F from Equation (5) using only daytime observations did not improve the correlations with τ_{atm}, showing that emission from nocturnal clouds is not the main source of error in Equation (8).

Air temperature varies little and humidity is high during cloudy periods. Table I shows linear correlations between the cloud emission factor (F) and RH, T and τ_{atm} on daily time scales. Relative humidity was the variable best correlated with cloud emissivity ($r^2 \sim 0{\cdot}5$–$0{\cdot}6$). Using specific humidity or water vapour pressure, instead of RH, slightly decreased the correlations. Shortwave transmissivity and temperature variance gave similar correlations with F ($r^2 \sim 0{\cdot}2$–$0{\cdot}4$). The daily amplitude of air temperature also gave similar results, but the amplitude is more sensitive to measurement errors than the variance, which incorporates all the measurements.

Multiple regressions of F with RH and τ_{atm} improved the calculations, as the resulting equation explained approximately 60% of the variation of cloud emissivity (Table I). The addition of T to this parameterization

DOI: 10.1002/hyp

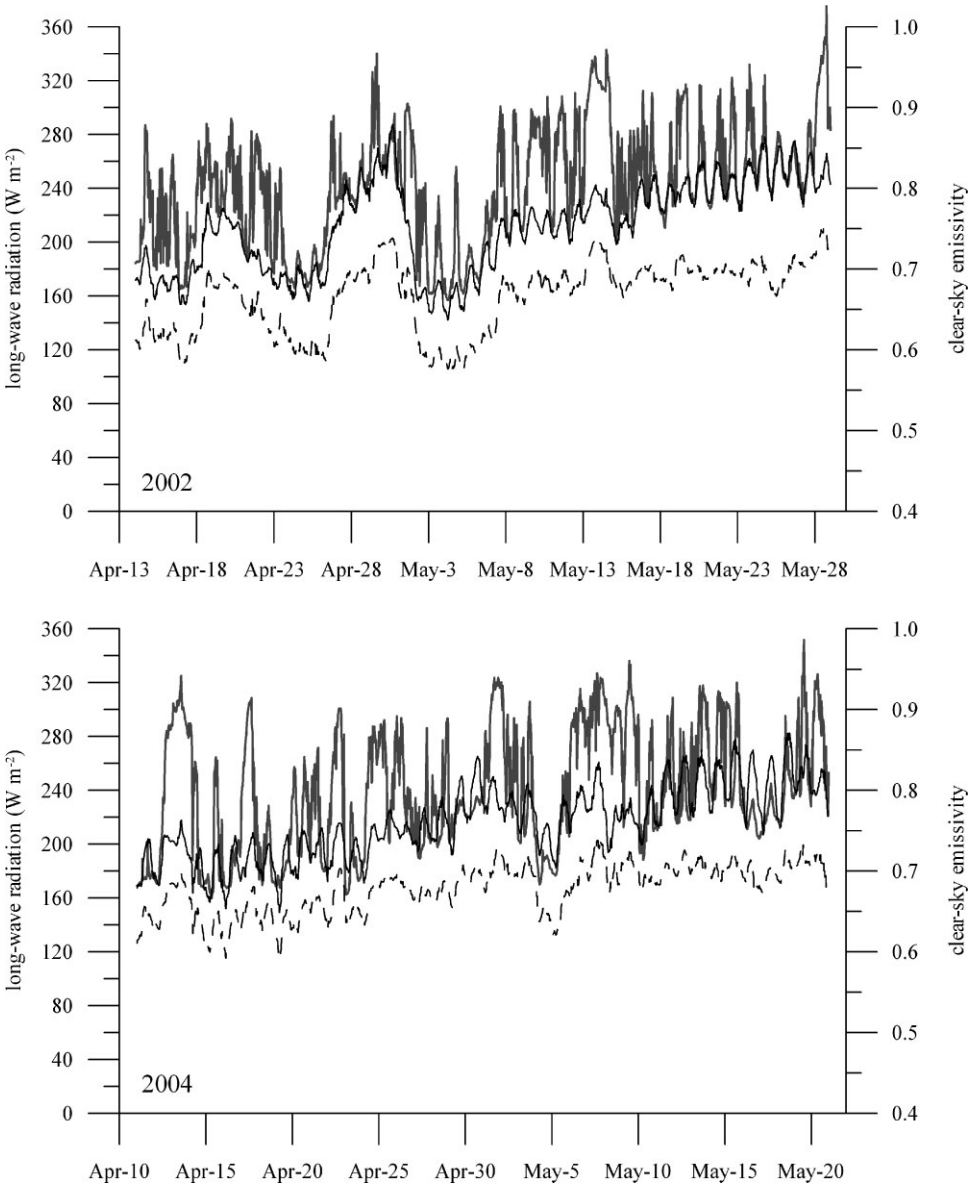

Figure 3. Half-hourly averages of longwave irradiance in 2002 (upper panel) and 2004 (lower panel), showing measurements (grey line) and calculated for clear skies according to Brutsaert (1975) (black line, Equation (2)). The dashed line shows calculated clear-sky emissivity (right Y axis)

did not significantly improve the regressions. The final parameterization for longwave irradiance in open environments is

$$L_0 = 1{\cdot}24\ (e/T)^{1/7}(1 + 0{\cdot}44\ RH - 0{\cdot}18\ \tau_{atm})\ \sigma\ T^4 \tag{9}$$

with e in millibars, T in Kelvin, RH and τ_{atm} as fractions, and $F = 1 + 0{\cdot}44\ RH - 0{\cdot}18\ \tau_{atm}$ comes from the regressions in 2002 and 2004. The variables e, T and RH are half-hourly averages, whereas τ_{atm} is a daily value.

As the factor F depends on the variables T and e (Equation (5)), the correlation coefficients $r(F, T)$ and $r(F, e)$ (Table I) may be artificially increased by 'spurious self-correlations' (Kenney, 1982). Fortunately, F

DOI: 10.1002/hyp

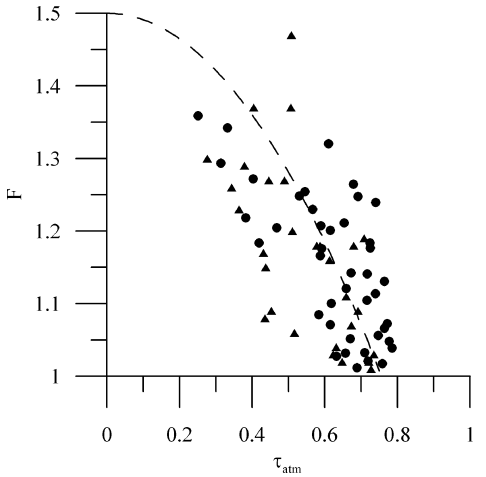

Figure 4. Increase of sky emissivity due to cloud emissions ($F = L_0/L_{0,\text{clear}}$) versus atmospheric solar transmissivity (τ_{atm}). The data are daily averages in spring 2002 (dots) and 2004 (triangles). The dashed line shows Equation (8)

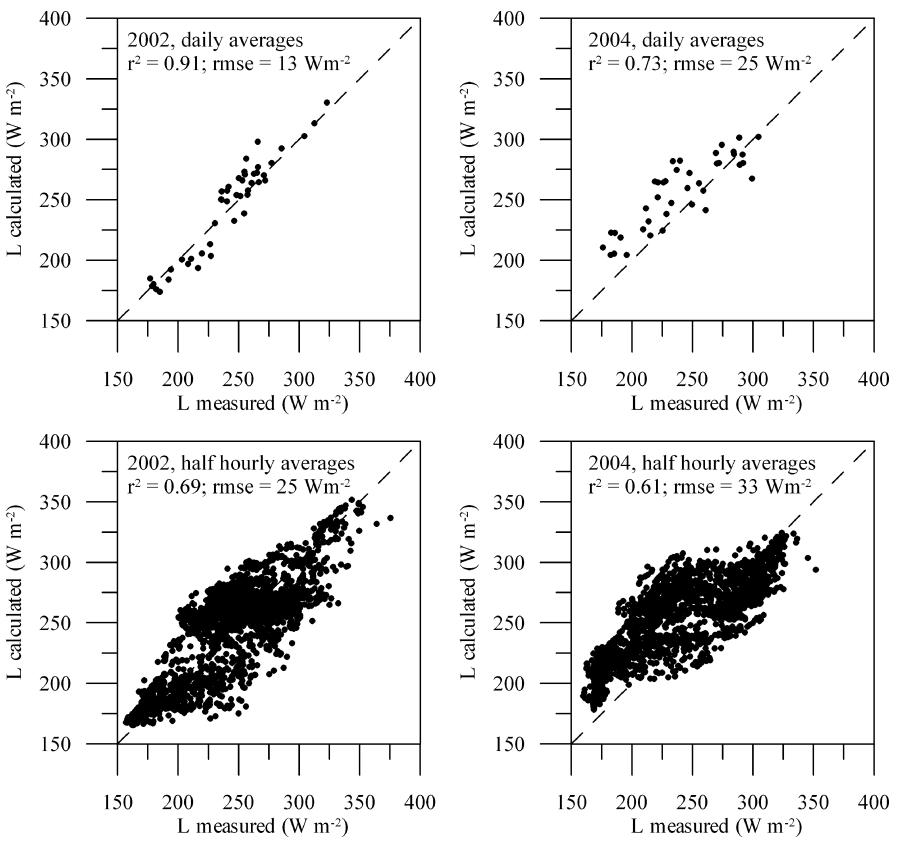

Figure 5. Longwave irradiance calculations (Equation (9)) versus measurements during spring 2002 and 2004

DOI: 10.1002/hyp

is calculated from τ_{atm} and RH (Equation (9)) and RH is poorly correlated to T and to e ($r^2 < 0{\cdot}1$). Thus, we can expect that spurious self-correlations have a small effect on the final parameterization of L.

Calculations were in fairly good agreement with the measurements on half-hourly and daily time scales (Figures 5 and 6), with a root mean square (rms) error less than 25 W m^{-2} (33 W m^{-2}) for daily (hourly) estimates. Equation (9) gave better results than Equation (8) with F derived only from shortwave atmospheric transmissivity. However, high peaks in L due to thick clouds were underestimated, whereas low nocturnal values were overestimated. As the cumulated error over spring was small (<10%), errors cancelled each other out.

Figure 7 shows an independent test of Equation (9) for a site near the city of Saskatoon. The calculation period was from late winter to the beginning of spring 2004 with a colder atmosphere than spring in Wolf Creek (Figure 1). The calculated clear-sky emissivity was often too low, but the total longwave irradiance was quite well simulated and the cumulated error over the period of study was very small (<5%), with an rms error of 29 W m^{-2} and an r^2 of 0·5.

DISCUSSION AND CONCLUSIONS

In high-latitude environments, longwave and shortwave radiation contribute similar amounts of energy over the snowmelt season, from 10 to 26 MJ m^{-2} day^{-1}. A sensitivity study defined conditions under which surrounding terrain emissions of longwave radiation increase irradiance at the snow surface. Terrain emission can be significant when the sky irradiance is low: in the cold and dry atmosphere of early spring, and at high elevations or latitudes. The emission from warm and snow-free south-facing slopes may enhance snowmelt on opposing north-facing slope: longwave irradiance can increase by up to 60% for valley slopes of 35°. For most northern mountainous environments ($V_f > 0{\cdot}6$), the total longwave irradiance is not very sensitive to the temperature of the emitting surfaces, which is difficult to estimate. In contrast, an accurate estimation of the sky view factor is crucial; a high spatial resolution is required in distributed snowmelt models.

Brutsaert's equation simulates the clear-sky longwave radiation in Wolf Creek on an hourly time scale with an accuracy of around ±15%, close to the measurement uncertainties. Changes in surface properties as snow cover is depleted may be associated with a change in the relationship between the meteorological

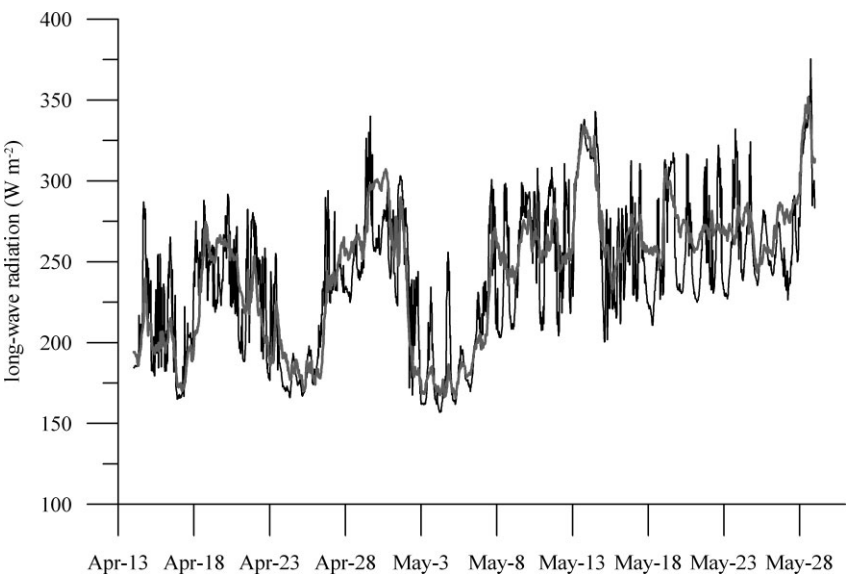

Figure 6. Longwave irradiance measurements (black line) and calculations (grey line) during spring 2002

DOI: 10.1002/hyp

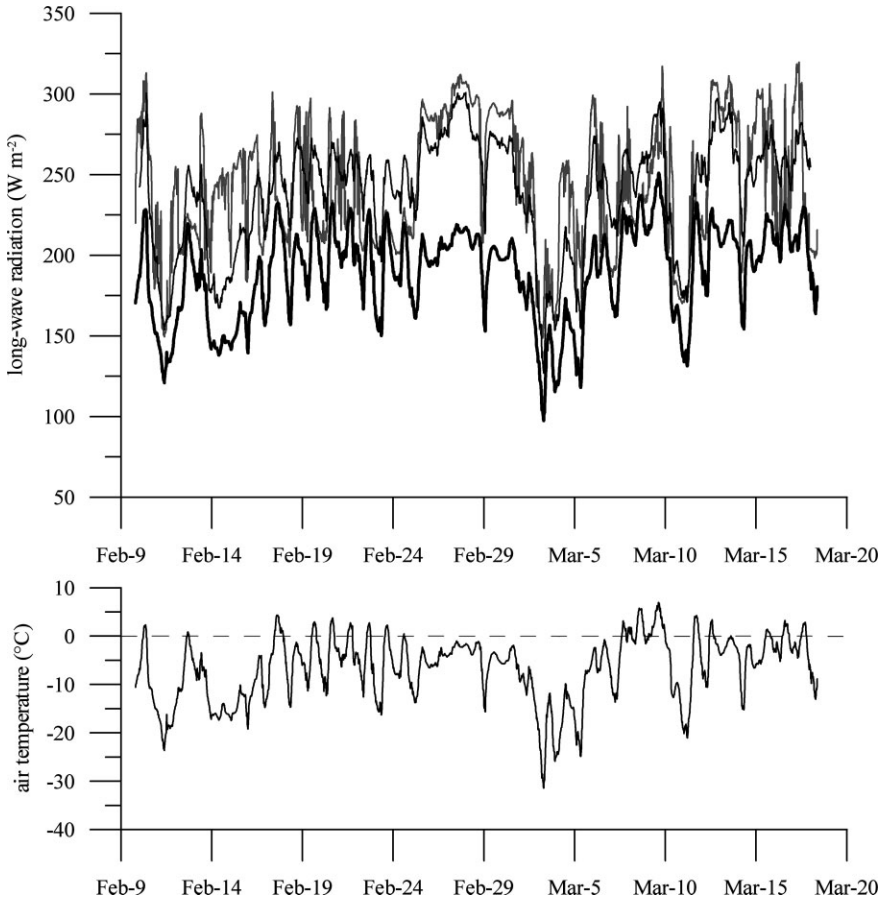

Figure 7. Upper panel shows longwave irradiance measurements (grey line) and calculations (black line). The thick line shows the clear-sky emission according to Brutsaert (1975). Lower panel shows air temperature (solid line). The data are hourly averages for Saskatoon during spring 2004

variables measured near the ground and the radiative properties of the atmosphere. However, there is no evidence of an increasing error in the longwave calculations as snow cover depletion progressed in Wolf Creek. Brutsaert's equation seems robust enough to be used unchanged throughout the entire snowmelt season. The error in longwave radiation measurements is maximal during clear-sky days, when solar radiation is high. However, the calibration of sky emissivity calculations on nighttime observations only, to reduce measurement errors (e.g. Swinbank, 1963), would bias the parameterization towards nocturnal inversion conditions.

On average during spring, clouds enhance the sky longwave radiation by about 16% in Wolf Creek. The maximal enhancement due to clouds was around 50%, but for 90% of the cloudy days the increase was less than 30%. The cloud emission factor was derived from multiple regressions with hourly air humidity (high in cloudy periods) and daily atmospheric shortwave transmissivity (small in cloudy periods). The daily variance of temperature (small in cloudy periods) did not add significant information, probably because of the correlation between temperature and humidity.

Atmospheric shortwave transmissivity does not account for nocturnal clouds, but cloud-cover does not change much over 24-h periods in Wolf Creek, so the error is small. The shortwave transmissivity index of clouds can also be perturbed by multiple reflections of solar radiation between the snow surface and the cloud

DOI: 10.1002/hyp

base, causing large solar irradiances under partly overcast skies that also have high longwave emissivities (Figure 4).

The calculations provide good estimates of longwave irradiance on daily time scales. The cumulated error over the snowmelt season is small, less than 10%, with little effect on total snowmelt calculations. On hourly time scales, the simulations dampen the variations of irradiance; peak values due to thick clouds are underestimated, whereas nocturnal minima are overestimated. The discrepancy is partly due to the summation of shortwave transmissivities over the sunshine hours. An independent test near the city of Saskatoon (52°7′N, 106°4′W) indicates that the calculations are robust in late winter, pre-melt conditions.

ACKNOWLEDGEMENTS

The authors would like to thank all those who contributed to the field experiments, especially Newell Hedstrom and Raoul Granger (Environment Canada), Michael Solohub and Steve McCartney (University of Saskatchewan), Rick Janowicz, Glen Ford and Glen Carpenter (Yukon Environment). Wolf Creek Research Basin is operated by the Water Resources Branch, Yukon Department of Environment and the National Water Research Institute, Environment Canada. This research project and J. E. Sicart were supported by the Natural Environment Research Council (UK) Standard Grant NER/A/S/2001/01089. The experiment was further supported by the Canadian Foundation for Climate and Atmospheric Sciences and the British Council.

REFERENCES

Ambach W. 1974. The influence of cloudiness on the net radiation balance of a snow surface with high albedo. *Journal of Glaciology* **13**: 73–84.

Brutsaert W. 1975. On a derivable formula for longwave radiation from clear skies. *Water Resources Research* **11**: 742–744.

Brutsaert W. 1982. *Evaporation into the Atmosphere, Theory, History and Applications*, 1st edn. Kluwer: Dordrecht; 1–299.

Culf AD, Gash JHC. 1993. Longwave radiation from clear skies in Niger: A comparison of observations with simple formulas. *Journal of Applied Meteorology* **32**: 539–547.

Dozier J, Warren SG. 1982. Effect of viewing angle on the infrared brightness temperature of snow. *Water Resources Research* **18**: 1424–1434.

Duguay CR. 1993. Radiation modeling in mountainous terrain review and status. *Mountain Research and Development* **13**: 339–357.

Fassnacht SR, Snelgrove KR, Soulis ED. 2001. Daytime longwave radiation approximation for physical hydrological modelling of snowmelt: a case study of southwestern Ontario. *Proceedings Sixth IAHS Scientific Assembly Symposium*, IAHS 270. IAHS: Maastricht; 279–286, July 2001.

Granger RJ, Gray DM. 1990. A net radiation model for calculating daily snowmelt in open environments. *Nordic Hydrology* **21**: 217–234.

Halldin S, Lindroth A. 1992. Errors in net radiometry: comparison and evaluation of six radiometer designs. *Journal of Atmospheric and Oceanic Technology* **9**: 762–783.

Kipp&Zonen. 1995. Instruction manual CNR1 net-radiometer, 1–42.

Kenney BC. 1982. Beware of spurious self-correlations!. *Water Resources Research* **18**: 1041–1048.

Konzelmann T, Van De Wal RSW, Greuell W, Bintanja R, Henneken EAC, Abe-Ouchi A. 1994. Parameterization of global and longwave incoming radiation for the Greenland Ice Sheet. *Global and Planetary Change* **9**: 143–164.

Marks D, Dozier J. 1979. A clear-sky longwave radiation model for remote Alpine areas. *Archives for Meteorology Geophysics and Bioclimatology Series B* **27**: 159–187.

Müller H. 1985. Review paper: On the radiation budget in the Alps. *Journal of Climatology* **5**: 445–462.

Obleitner F, De Wolde J. 1999. On intercomparaison of instruments used within the Vatnajökull glacio-meteorological experiment. *Boundary-Layer Meteorology* **92**: 27–37.

Oke TR. 1987. *Boundary Layer Climates*, 2nd edn. Routledge: New York; 1–435.

Olyphant GA. 1986. Longwave radiation in mountainous areas and its influence on the energy balance of Alpine snowfields. *Water Resources Research* **22**: 62–66.

Philipona R, Dutton EG, Stoffel T, Michalsky J, Reda I, Stifter A, Wendling P, Wood N, Clough SA, Mlawer EJ, Anderson G, Revercomb HE, Shippert T. 2004. Radiative forcing–measured at Earth's surface–corroborate the increasing greenhouse effect. *Geophysical Research Letters* **31**: L03202.

Plüss C, Ohmura A. 1997. Longwave radiation on snow-covered mountainous surfaces. *Journal of Applied Meteorology* **36**: 818–824.

Pomeroy JW, Granger RJ. 1997. *Sustainability of the Western Canadian Boreal Forest Under Changing Hydrological Conditions. I. Snow Accumulation and Ablation*, IAHS Publication No 240. *IAHS*: 237–242.

Pomeroy JW, Toth B, Granger RJ, Hedstrom NR, Essery RLH. 2003. Variations in surface energetics during snowmelt in a subarctic mountain catchment. *Journal of Hydrometeorology* **4**: 702–719.

DOI: 10.1002/hyp

Sicart JE, Wagnon P, Ribstein P. 2005. Atmospheric controls of the heat balance of Zongo Glacier (16 °S, Bolivia). *Journal of Geophysical Research* **110**(D12): Art. No. D12106. DOI: 10·1029/2004JD005732.
Sicart JE, Pomeroy JW, Essery RLH, Hardy J, Link T, Marks D. 2004. A sensitivity study of daytime net radiation during snowmelt to forest canopy and atmospheric conditions. *Journal of Hydrometeorology* **5**: 774–784.
Swinbank WC. 1963. Longwave radiation from clear skies. *Quarterly Journal of the Royal Meteorological Society* **89**: 339–348.
Warren SG, Hahn CJ, London J. 1985. Silmutaneous occurrence of different cloud types. *Journal of Climate and Applied Meteorology* **24**: 658–667.